


NLRP6 Induces Pyroptosis by Activation of Caspase-1 in Gingival Fibroblasts

Journal of Dental Research
2018, Vol. 97(12) 1391–1398
© International & American Associations
for Dental Research 2018
Article reuse guidelines:
sagepub.com/journals-permissions
DOI: 10.1177/0022034518775036
journals.sagepub.com/home/jdr

W. Liu^{1*} , J. Liu^{1*}, W. Wang¹, Y. Wang^{2,3}, and X. Ouyang¹

Abstract

NLRP6, a member of the nucleotide-binding domain, leucine-rich repeat-containing (NLR) innate immune receptor family, has been reported to participate in inflammasome formation. Activation of inflammasome triggers a caspase-1–dependent programmed cell death called pyroptosis. However, whether NLRP6 induces pyroptosis has not been investigated. In this study, we showed that NLRP6 overexpression activated caspase-1 and gasdermin-D and then induced pyroptosis of human gingival fibroblasts, resulting in release of proinflammatory mediators interleukin (IL)–1 β and IL-18. Moreover, NLRP6 was highly expressed in gingival tissue of periodontitis compared with healthy controls. *Porphyromonas gingivalis*, which is a commensal bacterium and has periodontopathic potential, induced pyroptosis of gingival fibroblasts by activation of NLRP6. Together, we, for the first time, identified that NLRP6 could induce pyroptosis of gingival fibroblasts by activation of caspase-1 and may play a role in periodontitis.

Keywords: periodontitis, pattern recognition receptors, cell death, *Porphyromonas gingivalis*, inflammasomes, flow cytometry

Introduction

Pyroptosis is a newly identified type of programmed cell death mediated by caspase-1 and gasdermin-D (GSDMD) (Shi et al. 2015). During pyroptosis, caspase-1 becomes activated and forms a protein complex with a cytosolic pattern recognition receptor (PRR, serves as a sensor molecule) and apoptosis-associated speck-like protein containing a caspase recruitment domain (ASC), which connects caspase-1 to cytosolic PRR (Miao et al. 2011). This complex, termed *inflammasome*, cleaves pro-interleukin (IL)–1 β and pro-IL-18 into their mature forms, thus playing a critical role in inflammation (Lamkanfi and Dixit 2014). Nucleotide-binding domain, leucine-rich repeat-containing receptors (NLRs) are a class of cytoplasmic PRRs. Several pathogens such as *Streptococcus pneumoniae*, *Listeria monocytogenes*, and *Candida albicans* were found to induce pyroptosis by activating NLR family members, including NLRP3 and NLRC4 (Sauer et al. 2010; Wellington et al. 2014; Kim et al. 2015). However, whether other NLR family members play a role in pyroptosis is poorly understood.

NLRP6 is a newly characterized cytosolic PRR member that contributes to regulating host defenses against microbes, inflammation, and tumorigenesis (Elinav et al. 2011; Normand et al. 2011; Anand et al. 2012). NLRP6 exhibits a tissue-specific expression pattern, with high levels in intestines, liver, kidney, and lung (Lech et al. 2010; Kempster et al. 2011). In vitro studies have demonstrated that NLRP6 participated in inflammasome formation and regulated IL-18 secretion (Grenier et al. 2002; Elinav et al. 2011). However, no literature shows the relationship between NLRP6 inflammasome and pyroptosis.

Periodontitis is an oral inflammatory disease that results from the immune response to pathogen invasion (Lourenco et al. 2014). Several NLRs, such as NOD1, NOD2, and NLRP3,

have been demonstrated to participate in periodontitis (Huang et al. 2015; Chaves de Souza et al. 2016; Marchesan et al. 2016). In this study, we used periodontitis as our model to investigate the relationship between NLRP6 and pyroptosis. NLRP6 expression in human gingival tissue from patients with chronic periodontitis and in gingival fibroblasts (GFs) stimulated by the periodontal pathogen *Porphyromonas gingivalis* was assessed. The type of cell death activated by NLRP6 overexpression was determined by transmission electron microscopy (TEM), caspase-1 inhibition, and flow cytometric analysis. Moreover, activation of caspase-1 signaling pathway as well as IL-1 β and IL-18 production were investigated by quantitative real-time polymerase chain reaction (qPCR) and Western blot analysis. Finally, small interference RNA (siRNA) targeting NLRP6 was introduced into GFs to reveal the function of NLRP6 in GFs pyroptosis.

¹Department of Periodontology, Peking University School and Hospital of Stomatology, Beijing, China

²Central Laboratory, Peking University School and Hospital of Stomatology, Beijing, China

³Biobank, Peking University School and Hospital of Stomatology, Beijing, China

*Authors contributing equally to this article.

A supplemental appendix to this article is available online.

Corresponding Authors:

Y. Wang, Central Laboratory, Peking University School and Hospital of Stomatology, 22 Zhongguancun South Avenue, Haidian District, Beijing 100081, China.

Email: kqwangyx@bjmu.edu.cn

X. Ouyang, Department of Periodontology, Peking University School and Hospital of Stomatology, 22 Zhongguancun South Avenue, Haidian District, Beijing 100081, China.

Email: kqouyangxy@bjmu.edu.cn

Materials and Methods

Sampling and Immunohistochemistry Assays

This study was approved by the Medical Ethics Committee at Peking University School of Stomatology (Ethics Approval No. PKUSSIRB-201522049). Gingival tissue specimens ($n = 18$) were obtained from age-matched (32–62 y) healthy subjects ($n = 9$) and patients with chronic periodontitis ($n = 9$). The inclusion and exclusion criteria are listed in Appendix Table 1. Protocols for collecting gingival biopsies and immunohistochemical staining were conducted as previously described (Liu et al. 2014). The dilution of NLRP6 antibody (Abcam) for immunohistochemical staining was 1:100.

Cell Culture

GFs were obtained from 4 healthy individuals (2 males and 2 females, aged 20 to 30 y [mean age, 24.7 y]) who underwent the third molar extraction at the Department of Oral and Maxillofacial Surgery in Peking University School and Hospital of Stomatology, with written informed consents. GFs were cultured and identified as previously described (Liu et al. 2014) and were used in all experiments at the fourth to eighth passages.

Infection with Adenovirus Carrying NLRP6 Expression Cassette

Adenovirus type 4 containing full-length NLRP6 (adv4-NLRP6) and control adv4 vectors were produced by GenePharma Co. GFs were placed in 60-mm dishes and grown to 70% to 80% confluence. Adenoviral infection was carried out at a multiplicity of infection (MOI) of 10:1 in the presence of polybrene (5 $\mu\text{g}/\text{mL}$) for 12 h.

Observation by Transmission Electron Microscope

Transmission electron microscopy was performed to confirm the type of cell death in GFs. Briefly, GFs were cultured in 60-mm dishes and infected with adv4-NLRP6 as described above. Cells were washed 3 times in phosphate-buffered saline (PBS), harvested with trypsin, and immediately centrifuged for 5 min at $5,000 \times g$. The cell pellets were washed twice with PBS and fixed with 2.5% glutaraldehyde. Transmission electron microscopy analysis was performed to observe the morphological change of GFs infected with adenovirus.

RNA Interference

NLRP6 small-interfering RNA and control siRNA were obtained from RiboBio Technology. Transfection of siRNA was performed by using Lipofectamine 3000 (Invitrogen), according to the manufacturer's instructions. A 100-pM siRNA was transfected into GFs for 48 h. The efficiency of the transfection and viability were also detected using Cy3-labeled transfection control. Both control and test groups were infected with *P. gingivalis*. The relative expression levels of NLRP6,

caspase-1, IL-1 β , and IL-18 were measured by qPCR and Western blot.

Bacterial Culture and Challenge

P. gingivalis strain W83 and *Enterococcus faecalis* strain 52199 were cultured as described in references (Ma et al. 2011; Wan et al. 2015). After growth for 24 h, bacteria were washed 3 times with PBS (pH, 7.2), measured at 600 nm, and then adjusted to an optical density of 0.5, corresponding to a concentration of 10^8 colony-forming units (CFU)/mL. Bacterial suspensions were added to confluent fibroblast monolayers at MOI of 50:1. At 8 h poststimulation, cells were then harvested and used in the following experiments.

Detection of Programmed Cell Death by Flow Cytometry

GFs exposed to adenovirus or *P. gingivalis* were washed twice with PBS. Caspase-1 inhibitor YVAD (Sigma-Aldrich) was used during infection as needed. Cells were labeled by FITC-coupled annexin V (annexin V-FITC) (BD Biosciences) for detection of phosphatidylserine exposure and by propidium iodide (PI) for observation of the loss of membrane integrity. Caspase-1 activity was measured by labeling with caspase-1-FITC from the FAM-FLICA caspase assay kits (Immunochemistry Technologies). Labeling was quantified using an Epics XL Flow Cytometer (Beckman Coulter). The rate of positive cells was used for comparison.

RNA Isolation and qPCR

Total RNA was isolated from cells using TRIzol reagent (Invitrogen) as described previously (Liu et al. 2014), and RNA concentration was measured by NanoDrop 8000 (Thermo Fisher Scientific). Reverse transcription was performed using a GoScript reverse transcription system (Promega) according to the manufacturer's protocol.

qPCR was performed in triplicate using an SYBR Green Reagent (Roche) and run on a ABI Prism 7500 Sequence Detection System (Applied Biosystems, Life Technologies). Primers for each gene are listed in Appendix Table 2. Standard PCR conditions were 10 min at 95°C, followed by 40 cycles of 95°C for 15 s and 60°C for 1 min. Glyceraldehyde-3-phosphate dehydrogenase (GAPDH) was taken as an endogenous control. Expression levels of target genes were calculated by a comparative $2^{-\Delta\Delta C_t}$ method after normalizing to GAPDH expression.

Western Blot Analysis

Cells were washed by PBS and lysed in 100 μL RIPA buffer (Applygen) containing proteinase and phosphatase inhibitors for 30 min on ice. The protein concentration was measured by a BCA Kit (Thermo Fisher Scientific). Then, proteins were separated by 10% sodium dodecyl sulfate polyacrylamide gel electrophoresis, transferred to polyvinylidene difluoride membranes, and blocked with 5% nonfat dry milk in TBST

(Tris-buffered saline plus Tween-20) for 1 h. Immunodetection was performed using antibodies against GAPDH (ZSbio; cat. SC-17790), NLRP6 (Abcam; cat. ab116007), caspase-1 (Cell Signaling Technology; cat. 2225S), and GSDMD (Abcam; cat. Ab155233) at 4°C overnight. After incubating with peroxidase-linked secondary antibodies, ECL Reagent (Thermo Fisher Scientific) was used to visualize immunoreactive proteins.

Cytokine Analysis

IL-1 β and IL-18 levels were measured using enzyme-linked immunosorbent assay (ELISA) kits from Neobioscience (cat. EHC002b, EHC127) according to the manufacturer's instruction. The samples were added to the 96-well plates and absorbance was measured at 450 nm.

Coimmunoprecipitation

Total proteins were isolated from GFs as stated above, incubated with 5 μ L anti-ASC (Santa Cruz; sc-514414) or anti-NLRP6 antibody at 4°C overnight, and then incubated with protein A + G agarose (Beyotime) for 2 h at 4°C. The samples were centrifuged at $2,500 \times g$, 5 min for 5 times to wash the magnetic beads. Immunoprecipitated proteins were then used for Western blot analysis to evaluate the expression and relationship of ASC and NLRP6.

Statistical Analysis

Data are expressed as the means \pm SD of at least 3 independent experiments. Student's *t* test and multivariate analysis of variance (ANOVA) of SPSS were used to determine the statistical significance of differences among each group. Level of significance (*P*) was set as <0.05 .

Results

Upregulation of NLRP6 Expression in Tissues with Periodontitis and *P. gingivalis*-stimulated GFs

To assess NLRP6 expression, gingival tissues from both periodontitis group and healthy group were sectioned and then stained with anti-NLRP6 antibody for immunohistochemistry. Compared with the number in the healthy group, the number of NLRP6-positive fibroblasts was significantly increased in the periodontitis group (Fig. 1A).

GFs were challenged by either a putative periodontal pathogen, *P. gingivalis*, or a control bacterium, *E. faecalis*. NLRP6 activation was verified by qPCR and Western blot analysis, and results showed that 2, 4, and 8 h after *P. gingivalis* infection, NLRP6 expression in GFs was upregulated at both messenger RNA (mRNA) and protein levels (Fig. 1B, C). However, NLRP6 expression was not significantly up-regulated by *E. faecalis* infection (Fig. 1D, E).

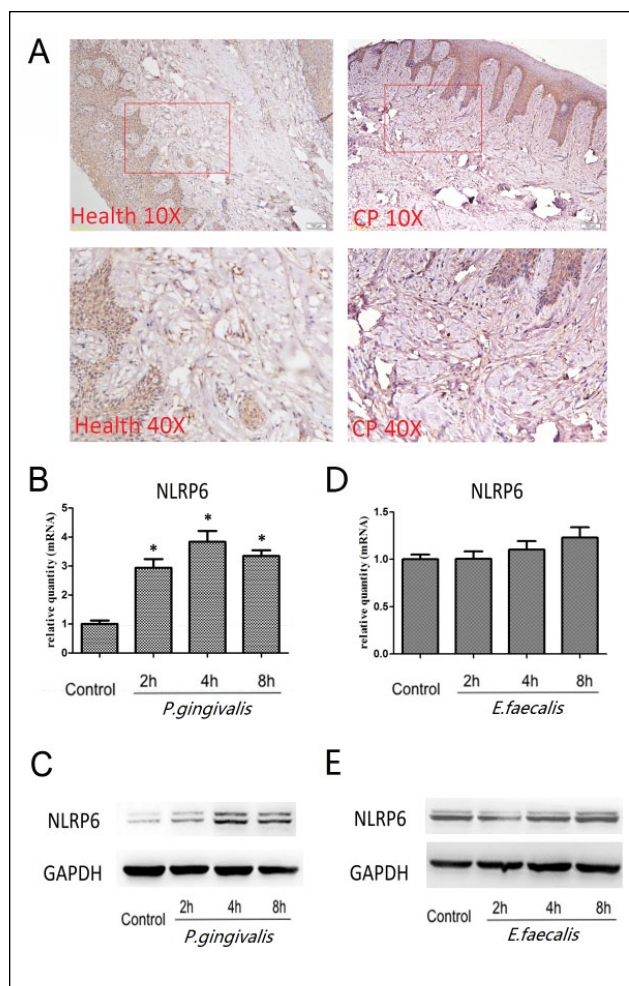


Figure 1. NLRP6 expression in gingival tissues and gingival fibroblasts (GFs). (A) Immunohistochemistry of gingival sections from healthy or periodontitis group using anti-NLRP6 antibody. (B) Detection of NLRP6 messenger RNA (mRNA) levels in GFs treated with *Porphyromonas gingivalis* W83 at multiplicity of infection (MOI) 50:1 for 2, 4, and 8 h. (C) Detection of NLRP6 protein levels in GFs treated with *P. gingivalis* W83 at MOI 50:1 for 2, 4, and 8 h. (D) Detection of NLRP6 mRNA levels in GFs treated with *Enterococcus faecalis* at MOI 50:1 for 2, 4, and 8 h. (E) Detection of NLRP6 protein levels in GFs treated with *E. faecalis* at MOI 50:1 for 2, 4, and 8 h. **P* < 0.05 compared with their corresponding untreated controls.

Pyroptosis-Like Morphological Changes of GFs Infected with NLRP6 Adenovirus

Typical pyroptosis morphology has been defined as cellular, nuclear, and mitochondrial swelling; pore formation; and early disruption of the plasma membrane. To further elucidate the impact of NLRP6 activation on GFs, an adenovirus carrying an NLRP6 expression cassette was used to infect GFs. Significant cell death was observed by optical microscopy at 12 h after infection (Appendix Fig. 1). The TEM results showed that GFs infected with adv4-NLRP6 displayed hallmarks of pyroptotic cell death (cell swelling and membrane rupture) with the

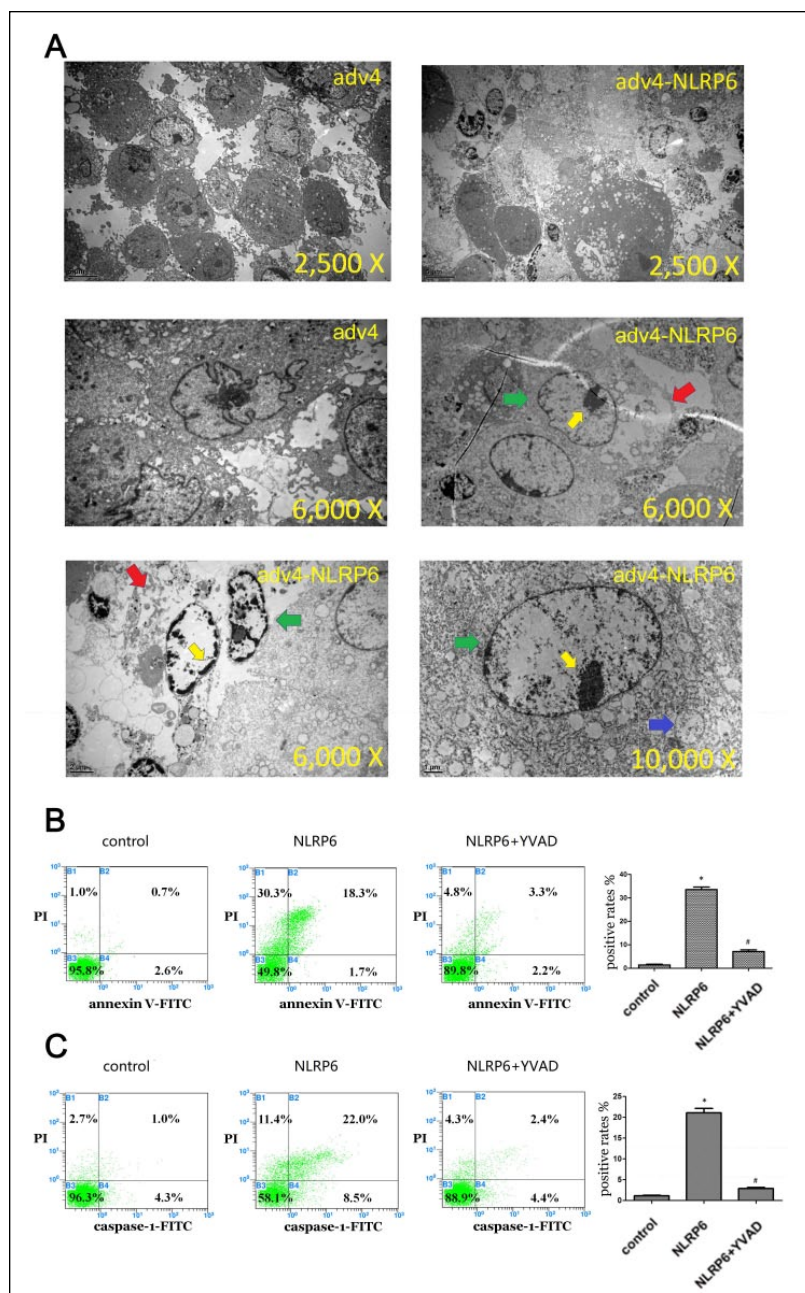


Figure 2. Detection of pyroptosis in gingival fibroblasts (GFs) infected with adv4 or adv4-NLRP6. GFs were infected with adv4-NLRP6 for 12 h and infected with adv4 only as a control group; Ac-YVAD-cMK was simultaneously added to the NLRP6-YVAD group. (A) Transmission electron microscopy observation of GFs infected with adv4 or adv4-NLRP6. Pyroptotic GFs show membrane rupture (red arrow) as well as chromatin margination and condensation (yellow arrow); nuclei (green arrow) and mitochondria (blue arrow) remain intact but exhibit swelling. (B) Cells were stained with propidium iodide (PI) and annexin V-FITC for flow cytometric analysis. (C) Cells were stained with PI and caspase-1-FITC for flow cytometric analysis. * $P < 0.05$ compared with control group; # $P < 0.05$ compared with NLRP6 group.

absence of apoptotic morphological features (cell shrinkage and intact membrane) (Fig. 2A). Chromatin margination and condensation are characteristics of the nucleus shared between apoptosis and pyroptosis, but there were no signs of karyorrhexis or apoptotic bodies found.

Flow Cytometry Confirms That NLRP6 Activates Pyroptosis in GFs and Is Dependent on Caspase-1 Activation

Flow cytometric analysis of cells by double-labeled annexin V-FITC and PI showed that the number of PI-positive GFs was significantly increased while adv4-NLRP6 infection indicated the loss of cell membrane integrity. The results showed that few apoptotic-like cells (annexin-V+/PI-) were detected. Because pyroptosis was defined as caspase-1-dependent cell death, we detected the portion of pyroptotic cells by adding a caspase-1-specific inhibitor, Ac-YVAD-cMK (YVAD), at the time of adenoviral infection. Compared to the NLRP6 group, the number of PI-positive GFs in the NLRP6 + YVAD group was significantly reduced (Fig. 2B). We then double-labeled cells with caspase-1-FITC and PI, and flow cytometric analysis showed that most caspase-1-FITC-positive cells were also PI positive (Fig. 2C), thus indicating that caspase-1 is strongly linked to this type of cell death. In addition, YVAD significantly reduced the proportion of cells stained with PI and caspase-1-FITC. Based on the definition of pyroptosis, we verified that the cell death induced by adv4-NLRP6 was caspase-1-dependent pyroptosis.

NLRP6 Interacts with ASC and Induces the Release of Inflammatory Mediators IL-1 β and IL-18 by Activating Caspase-1

To investigate whether NLRP6 activates inflammasome pathway, coimmunoprecipitation assays were performed. Proteins were precipitated by either an anti-ASC antibody or anti-NLRP6, and then precipitates were used for Western blot analysis. ASC-NLRP6 was more effectively coprecipitated in GFs infected by adv4-NLRP6 than GFs infected with adv4 control virus only (Fig. 3A). While the inflammasome pathway was activated, a p20 subunit cleaved from pro-caspase-1, pro-GSDMD was also cleaved to generate an N-terminal product (GSDMD-NT) that formed pores in membranes and triggered pyroptosis. Western blot results demonstrated that pro-caspase-1 and pro-GSDMD were cleaved in adv4-NLRP6-infected GFs, and these cleavage events were inhibited by YVAD (Fig. 3B). IL-1 β and IL-18 released by NLRP6 overexpression were examined by qPCR and ELISA analysis. The results showed that the expression levels of IL-1 β and IL-18 were elevated by

adv4-NLRP6 infection at both mRNA and protein levels. However, upregulation of IL-1 β and IL-18 was reduced by YVAD (Fig. 3C, D). These results demonstrated that IL-1 β and IL-18 secretion and GSDMD cleavage in adv4-NLRP6-infected GFs depended on caspase-1.

P. gingivalis–Induced Cell Death and *P. gingivalis*–Mediated Release of IL-1 β and IL-18 Are Attenuated by NLRP6 Knockdown

To further determine whether NLRP6 mediates the inflammasome pathway during *P. gingivalis* infection, scramble siRNA (siCON) or NLRP6 siRNA (siNLRP6) were transfected into GFs 48 h before *P. gingivalis* W83 infection. Flow cytometric results showed that PI- and caspase-1–positive cells were increased under *P. gingivalis* infection (Fig. 4A-a, b). While YVAD were added at the time of infection, PI- and caspase-1–positive cells were partially reduced (Fig. 4A-c). This result indicated that a proportion of GFs might undergo pyroptosis in the presence of *P. gingivalis*. Downregulation of NLRP6 clearly attenuated the expression of PI- and caspase-1–positive cells during *P. gingivalis* infection (Fig. 4A-d). These results verified that the induction of pyroptosis by *P. gingivalis* is dependent on NLRP6.

qPCR showed *P. gingivalis* induced expression of caspase-1, IL-1 β , and IL-18 at the mRNA level, and the expression of these genes was inhibited by both NLRP6 siRNA and YVAD (Fig. 4B). Western blot demonstrated that pro-caspase-1 and pro-GSDMD were cleaved during *P. gingivalis* infection (Fig. 4C). ELISA analysis showed that the secretion of IL-1 β and IL-18 were stimulated by *P. gingivalis* infection (Fig. 4D). Moreover, either YVAD or NLRP6 siRNA significantly inhibited these effects of *P. gingivalis* (Fig. 4B–D). Knockdown efficiency of siNLRP6 was evaluated by qPCR (Fig. 4E).

Discussion

Previous studies showed that several NLR inflammation complexes could trigger pyroptosis. Known NLRs involved in pyroptosis were limited to NLRP3, NLRC4, NLRP1b, and NLRP9 (Ahn et al. 2017; Zhu et al. 2017; Wu et al. 2018; Zhao et al. 2018). In our preliminary experiment, the NLR family expression in gingival tissue has been detected by microarray assay and validated by qPCR (Appendix Fig. 2). Results showed that NLRP6 expression was upregulated in the periodontitis group compared with the healthy group while other NLR family members' expression changed insignificantly. Our experiments then revealed that activation of the NLRP6 inflammasome in GFs could also lead to pyroptosis. To our knowledge, this study elucidates the relationship between the NLRP6 inflammasome and pyroptosis for the first time.

Both apoptosis and pyroptosis are programmed cell death. In this study, we noticed that adv4-NLRP6–infected GFs exhibited pyroptotic morphological features by TEM (cytoplasmic, nuclear, and mitochondrial swelling; membrane rupture;

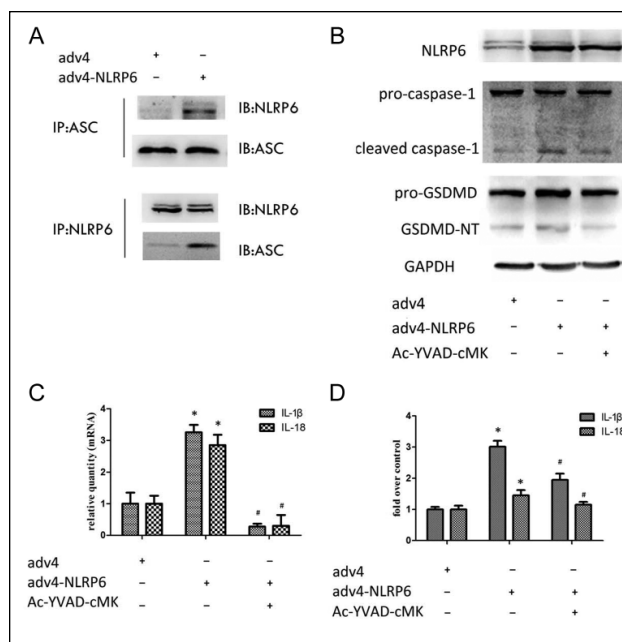


Figure 3. Detection of apoptosis-associated speck-like protein containing a caspase recruitment domain (ASC), caspase-1, interleukin (IL)–1 β , IL-18, and gasdermin-D (GSDMD) in gingival fibroblasts (GFs) infected with adv4 or adv4-NLRP6. GFs were infected with adv4 or adv4-NLRP6 for 12 h. Ac-YVAD-cMK was simultaneously added to the NLRP6-YVAD group. (A) Proteins were immunoprecipitated with an anti-ASC or anti-NLRP6 antibody and measured by Western blot analysis. (B) Expression of NLRP6 and cleavage of pro-caspase-1 and pro-GSDMD were measured by Western blot analysis. (C) Messenger RNA expression levels of IL-1 β and IL-18 were analyzed by quantitative real-time polymerase chain reaction (qPCR). (D) Enzyme-linked immunosorbent assay (ELISA) of secreted IL-1 β and IL-18 in the media of cells treated as indicated. * $P < 0.05$ compared with adv4 group; # $P < 0.05$ compared with adv4-NLRP6 group.

and chromatin condensation). In contrast, apoptosis is characterized by cell shrinkage, DNA fragmentation into nucleosome-size fragments called apoptotic bodies, phosphatidylserine externalization, and eventual engulfment by phagocytes or surrounding cells (Balvan et al. 2015). Membrane-impermeant dyes, such as PI, stain pyroptotic cells but not apoptotic cells at early phases. However, annexin V could stain apoptotic cells due to exposed phosphatidylserine and pyroptotic cells due to membrane pore formation (Edgeworth et al. 2002; Miao et al. 2011). From the above data, pyroptotic cells were PI+/annexin V+, while apoptotic cells were PI–/annexin V+. Pyroptosis is first defined by its initial dependence on caspase-1, but apoptosis occurs after caspase-8/-9/-3 activation (Martinon et al. 2002; Xiao et al. 2012; Hsiao et al. 2014). The differences between apoptosis and pyroptosis are listed in the Table. Together, flow cytometric analysis and the effectiveness of the caspase-1 inhibitor demonstrated that NLRP6 overexpression induced the pyroptotic cell death pathway.

Most studies of NLRP6 have focused on its function in intestinal microbial regulation (Wlodarska et al. 2014; Levy et al. 2015; Birchenough et al. 2016). In this study, NLRP6 was also found to be expressed in human gingival connective tissue and to act as a proinflammatory mediator in GFs. Activation of

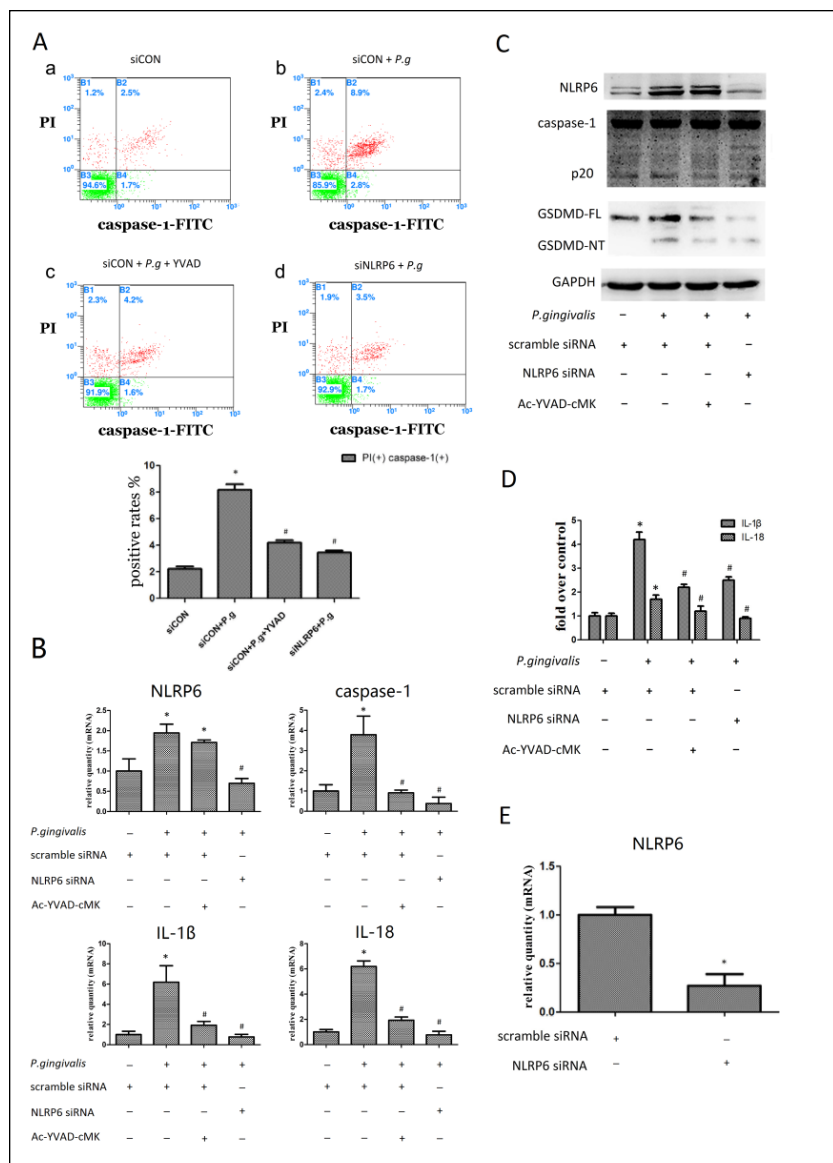


Figure 4. Pyroptosis detection in *Porphyromonas gingivalis*-infected gingival fibroblasts (GFs) with or without NLRP6 gene knockdown. (A) Flow cytometric analysis of GFs by propidium iodide (PI) and caspase-1-FITC staining. (B) Messenger RNA (mRNA) expression levels of NLRP6, caspase-1, interleukin (IL)-1β, and IL-18 were measured by quantitative real-time polymerase chain reaction (qPCR). (C) Expression of NLRP6 and cleavage of pro-caspase-1 and pro-gasdermin-D (GSDMD) were measured by Western blot analysis. (D) Enzyme-linked immunosorbent assay (ELISA) of secreted IL-1β and IL-18 in the media. (E) mRNA knockdown efficiency of siNLRP6. *P < 0.05 compared with control group; #P < 0.05 compared with NLRP6 group.

NLRP6 in GFs increased the production of mature IL-1β and IL-18 and triggered pyroptosis. IL-1β and IL-18 are both critical inflammatory mediators of periodontitis. IL-1β is known to activate lymphocytes and macrophages, regulate the production of many cytokines, and promote osteoclast formation and bone resorption (Graves and Cochran 2003; Lee et al. 2010). IL-1β levels in gingival tissues have been found to correspond

to periodontal status, suggesting its levels may reflect disease severity (Oh et al. 2015). In addition, IL-18 has been found to induce the release of MMP-9, activate macrophages, and promote neutrophils to upregulate the production of IL-1β (Reddy et al. 2010; Valente et al. 2012; Ketelut-Carneiro et al. 2015). As pyroptosis occurs, 10- to 15-nm pores form in the cell membrane, thus enabling the release of cytoplasmic content, including invading pathogens and inflammatory cytokines, resulting in recruiting more inflammatory cells to drive the inflammatory cascades and eliminate the pathogens (Ding et al. 2016; Sborgi et al. 2016). Moreover, siNLRP6 may block the inflammasome pathway, leading to inhibiting a series of consequences of pyroptosis. Above all, our new findings elucidate that NLRP6 plays an imperative role in defending against microbial infection and in regulating the immune response, which indicates a new mechanism for the pathogenesis of periodontitis.

In addition, YVAD is a peptide inhibitor of caspase-1. But when YVAD is added, the mRNA level of caspase-1 is not upregulated by either adv4-NLRP6 or *P. gingivalis* infection. We speculate that YVAD inhibits the oligomerization of caspase-1, ASC, and NLRP6 and interferes with inflammasome formation, finally leading to an unchanged caspase-1 mRNA expression level after infection.

P. gingivalis is one of the major pathogens associated with chronic periodontitis. Desta and Graves (2007) have found that *P. gingivalis* infection induced apoptosis in GFs, but our study revealed the simultaneous existence of pyroptosis. In addition, we noticed that cell death induced by adv4-NLRP6 was not completely activated by caspase-1, which indicates that, beyond pyroptosis, NLRP6 may be involved in other types of cell death in periodontal fibroblasts. Since emerging evidence suggests that there are interactions between

different inflammatory responses and types of cell death, this study reminds us that NLRP6 might be part of this crosstalk (Lawlor et al. 2015). Moreover, various NLRP inflammasomes will work simultaneously to form such a network. Therefore, the overall function of NLRP6 and how it works together with these PRR signals in periodontitis should be clarified in the future.

Table. Comparison of Apoptosis and Pyroptosis.

Characteristics	Apoptosis	Pyroptosis
Membrane	Integrity	Disruption
Nuclear	DNA fragmentation apoptotic body	Swelling
Inflammasome	Caspase-3/-8/-9	Caspase-1/-4 in humans, caspase-1 in mice
Flow cytometry	PI-/annexin V+, PI+/ annexin V+ at later period	PI+/annexin V+ at early phase
Inflammation	Rare	Frequent

PI, propidium iodide.

Conclusion

The present study demonstrates that NLRP6 is upregulated in gingival tissue in periodontitis and participates in *P. gingivalis*-induced pyroptosis. Moreover, NLRP6 overexpression in GFs triggers pyroptosis, which results in IL-1 β and IL-18 secretion. These findings indicate a new mechanism in the pathogenesis of periodontitis, and NLRP6 can be considered a potential candidate for periodontal therapy.

Author Contributions

W. Liu, X. Ouyang, contributed to conception, design, data acquisition, analysis, and interpretation, drafted and critically revised the manuscript; J. Liu, contributed to conception, design, and data acquisition, drafted and critically revised the manuscript; W. Wang, contributed to conception and data analysis, drafted and critically revised the manuscript; Y. Wang, contributed to design, data acquisition, analysis, and interpretation, drafted and critically revised the manuscript. All authors gave final approval and agree to be accountable for all aspects of the work.

Acknowledgments

This study was supported by the National Natural Science Foundation of China grants (81271150, 81772873), Beijing Natural Science Foundation grants (7172240, 7182181), and the Peking University School of Stomatology Science Foundation (PKUSS20150103). The authors declare no potential conflicts of interest with respect to the authorship and/or publication of this article.

ORCID iD

W. Liu  <https://orcid.org/0000-0002-7332-9881>

References

Ahn H, Kang SG, Yoon SI, Ko HJ, Kim PH, Hong EJ, An BS, Lee E, Lee GS. 2017. Methylene blue inhibits NLRP3, NLRC4, AIM2, and non-canonical inflammasome activation. *Sci Rep.* 7(1):12409.

Anand PK, Malireddi RK, Lukens JR, Vogel P, Bertin J, Lamkanfi M, Kanneganti TD. 2012. NLRP6 negatively regulates innate immunity and host defence against bacterial pathogens. *Nature.* 488(7411):389–393.

Balvan J, Krizova A, Gumulec J, Raudenska M, Sladek Z, Sedlackova M, Babula P, Sztalmachova M, Kizek R, Chmelik R, et al. 2015. Multimodal holographic microscopy: distinction between apoptosis and oncosis. *PLoS One.* 10(3):e0121674.

Birchenough GM, Nystrom EE, Johansson ME, Hansson GC. 2016. A sentinel goblet cell guards the colonic crypt by triggering Nlrp6-dependent Muc2 secretion. *Science.* 352(6293):1535–1542.

Chaves de Souza JA, Frasnelli SC, Curylofo-Zotti FA, Avila-Campos MJ, Spolidorio LC, Zamboni DS, Graves DT, Rossa C Jr. 2016. NOD1 in the modulation of host-microbe interactions and inflammatory bone resorption in the periodontal disease model. *Immunology.* 149(4):374–385.

Desta T, Graves DT. 2007. Fibroblast apoptosis induced by *Porphyromonas gingivalis* is stimulated by a gingipain and caspase-independent pathway that involves apoptosis-inducing factor. *Cell Microbiol.* 9(11):2667–2675.

Ding J, Wang K, Liu W, She Y, Sun Q, Shi J, Sun H, Wang DC, Shao F. 2016. Pore-forming activity and structural autoinhibition of the gasdermin family. *Nature.* 535(7610):111–116.

Edgeworth JD, Spencer J, Phalipon A, Griffin GE, Sansonetti PJ. 2002. Cytotoxicity and interleukin-1 β processing following *Shigella flexneri* infection of human monocyte-derived dendritic cells. *Eur J Immunol.* 32(5):1464–1471.

Elinav E, Strowig T, Henao-Mejia J, Flavell RA. 2011. Regulation of the anti-microbial response by NLR proteins. *Immunity.* 34(5):665–679.

Graves DT, Cochran D. 2003. The contribution of interleukin-1 and tumor necrosis factor to periodontal tissue destruction. *J Periodontol.* 74(3):391–401.

Grenier JM, Wang L, Manji GA, Huang WJ, Al-Garawi A, Kelly R, Carlson A, Merriam S, Lora JM, Briskin M, et al. 2002. Functional screening of five PYPAF family members identifies PYPAF5 as a novel regulator of NF-kappaB and caspase-1. *FEBS Lett.* 530(1–3):73–78.

Hsiao PC, Lee WJ, Yang SF, Tan P, Chen HY, Lee LM, Chang JL, Lai GM, Chow JM, Chien MH. 2014. Nobiletin suppresses the proliferation and induces apoptosis involving MAPKs and caspase-8/-9/-3 signals in human acute myeloid leukemia cells. *Tumour Biol.* 35(12):11903–11911.

Huang X, Yang X, Ni J, Xie B, Liu Y, Xuan D, Zhang J. 2015. Hyperglucose contributes to periodontitis: involvement of the NLRP3 pathway by engaging the innate immunity of oral gingival epithelium. *J Periodontol.* 86(2):327–335.

Kempster SL, Belteki G, Forhead AJ, Fowden AL, Catalano RD, Lam BY, McFarlane I, Charnock-Jones DS, Smith GC. 2011. Developmental control of the Nlrp6 inflammasome and a substrate, IL-18, in mammalian intestine. *Am J Physiol Gastrointest Liver Physiol.* 300(2):G253–G263.

Ketelut-Carneiro N, Silva GK, Rocha FA, Milanezi CM, Cavalcanti-Neto FF, Zamboni DS, Silva JS. 2015. IL-18 triggered by the Nlrp3 inflammasome induces host innate resistance in a pulmonary model of fungal infection. *J Immunol.* 194(9):4507–4517.

Kim JY, Paton JC, Briles DE, Rhee DK, Pyo S. 2015. Streptococcus pneumoniae induces pyroptosis through the regulation of autophagy in murine microglia. *Oncotarget.* 6(42):44161–44178.

Lamkanfi M, Dixit VM. 2014. Mechanisms and functions of inflammasomes. *Cell.* 157(5):1013–1022.

Lawlor KE, Khan N, Mildenhall A, Gerlic M, Croker BA, D’Cruz AA, Hall C, Kaur Spall S, Anderton H, Masters SL, et al. 2015. RIPK3 promotes cell death and NLRP3 inflammasome activation in the absence of MLKL. *Nat Commun.* 6:6282.

Lech M, Avila-Ferrufino A, Skuginna V, Susanti HE, Anders HJ. 2010. Quantitative expression of RIG-like helicase, NOD-like receptor and inflammasome-related mRNAs in humans and mice. *Int Immunol.* 22(9):717–728.

Lee YM, Fujikado N, Manaka H, Yasuda H, Iwakura Y. 2010. IL-1 plays an important role in the bone metabolism under physiological conditions. *Int Immunol.* 22(10):805–816.

Levy M, Thaiss CA, Zeevi D, Dohnalova L, Zilberman-Schapira G, Mahdi JA, David E, Savidor A, Korem T, Herzig Y, et al. 2015. Microbiota-modulated metabolites shape the intestinal microenvironment by regulating NLRP6 inflammasome signaling. *Cell.* 163(6):1428–1443.

Liu J, Duan J, Wang Y, Ouyang X. 2014. Intracellular adhesion molecule-1 is regulated by *Porphyromonas gingivalis* through nucleotide binding oligomerization domain-containing proteins 1 and 2 molecules in periodontal fibroblasts. *J Periodontol.* 85(2):358–368.

Lourenco TG, Heller D, Silva-Boghossian CM, Cotton SL, Paster BJ, Colombo AP. 2014. Microbial signature profiles of periodontally healthy and diseased patients. *J Clin Periodontol.* 41(11):1027–1036.

Ma Z, Wang Y, Zhu X, Zhang C, Li S, Jin L, Shen Y, Haapasalo M. 2011. Role of polymorphonuclear neutrophils in the clearance of *Enterococcus faecalis* derived from saliva and infected root canals. *J Endod.* 37(3):346–352.

Marchesan J, Jiao Y, Schaff RA, Hao J, Morelli T, Kinney JS, Gerow E, Sheridan R, Rodrigues V, Paster BJ, et al. 2016. TLR4, NOD1 and NOD2 mediate immune recognition of putative newly identified periodontal pathogens. *Mol Oral Microbiol.* 31(3):243–258.

- Martinon F, Burns K, Tschopp J. 2002. The inflammasome: a molecular platform triggering activation of inflammatory caspases and processing of proIL-beta. *Mol Cell*. 10(2):417-426.
- Miao EA, Rajan JV, Aderem A. 2011. Caspase-1-induced pyroptotic cell death. *Immunol Rev*. 243(1):206-214.
- Normand S, Delanoye-Crespin A, Bressenot A, Huot L, Grandjean T, Peyrin-Biroulet L, Lemoine Y, Hot D, Chamaillard M. 2011. Nod-like receptor pyrin domain-containing protein 6 (NLRP6) controls epithelial self-renewal and colorectal carcinogenesis upon injury. *Proc Natl Acad Sci USA*. 108(23):9601-9606.
- Oh H, Hirano J, Takai H, Ogata Y. 2015. Effects of initial periodontal therapy on interleukin-1 β level in gingival crevicular fluid and clinical periodontal parameters. *J Oral Sci*. 57(2):67-71.
- Reddy VS, Prabhu SD, Mummidi S, Valente AJ, Venkatesan B, Shanmugam P, Delafontaine P, Chandrasekar B. 2010. Interleukin-18 induces EMMPRIN expression in primary cardiomyocytes via JNK/Sp1 signaling and MMP-9 in part via EMMPRIN and through AP-1 and NF-kappaB activation. *Am J Physiol Heart Circ Physiol*. 299(4):H1242-H1254.
- Sauer JD, Witte CE, Zemansky J, Hanson B, Lauer P, Portnoy DA. 2010. *Listeria monocytogenes* triggers AIM2-mediated pyroptosis upon infrequent bacteriolysis in the macrophage cytosol. *Cell Host Microbe*. 7(5):412-419.
- Sborgi L, Ruhl S, Mulvihill E, Pipercevic J, Heilig R, Stahlberg H, Farady CJ, Muller DJ, Broz P, Hiller S. 2016. GSDMD membrane pore formation constitutes the mechanism of pyroptotic cell death. *EMBO J*. 35(16):1766-1778.
- Shi J, Zhao Y, Wang K, Shi X, Wang Y, Huang H, Zhuang Y, Cai T, Wang F, Shao F. 2015. Cleavage of GSDMD by inflammatory caspases determines pyroptotic cell death. *Nature*. 526(7575):660-665.
- Valente AJ, Yoshida T, Murthy SN, Sakamuri SS, Katsuyama M, Clark RA, Delafontaine P, Chandrasekar B. 2012. Angiotensin II enhances AT1-Nox1 binding and stimulates arterial smooth muscle cell migration and proliferation through AT1, Nox1, and interleukin-18. *Am J Physiol Heart Circ Physiol*. 303(3):H282-H296.
- Wan M, Liu JR, Wu D, Chi XP, Ouyang XY. 2015. E-selectin expression induced by *Porphyromonas gingivalis* in human endothelial cells via nucleotide-binding oligomerization domain-like receptors and Toll-like receptors. *Mol Oral Microbiol*. 30(5):399-410.
- Wellington M, Koselny K, Sutterwala FS, Krysan DJ. 2014. *Candida albicans* triggers NLRP3-mediated pyroptosis in macrophages. *Eukaryot Cell*. 13(2):329-340.
- Wlodarska M, Thaiss CA, Nowarski R, Henao-Mejia J, Zhang JP, Brown EM, Frankel G, Levy M, Katz MN, Philbrick WM, et al. 2014. NLRP6 inflammasome orchestrates the colonic host-microbial interface by regulating goblet cell mucus secretion. *Cell*. 156(5):1045-1059.
- Wu X, Zhang H, Qi W, Zhang Y, Li J, Li Z, Lin Y, Bai X, Liu X, Chen X, et al. 2018. Nicotine promotes atherosclerosis via ROS-NLRP3-mediated endothelial cell pyroptosis. *Cell Death Dis*. 9(2):171.
- Xiao F, Gao W, Wang X, Chen T. 2012. Amplification activation loop between caspase-8 and -9 dominates artemisinin-induced apoptosis of ASTC-a-1 cells. *Apoptosis*. 17(6):600-611.
- Zhao LR, Xing RL, Wang PM, Zhang NS, Yin SJ, Li XC, Zhang L. 2018. NLRP1 and NLRP3 inflammasomes mediate LPS/ATP-induced pyroptosis in knee osteoarthritis. *Mol Med Rep*. 17(4):5463-5469.
- Zhu S, Ding S, Wang P, Wei Z, Pan W, Palm NW, Yang Y, Yu H, Li HB, Wang G, et al. 2017. Nlrp9b inflammasome restricts rotavirus infection in intestinal epithelial cells. *Nature*. 546(7660):667-670.